Available online at www.sciencedirect.com
ScienceDirect
Ceramics International 35 (2009) 1473–1480
CERAMICS INTERNATIONAL
www.elsevier.com/locate/ceramint

High temperature dielectric properties of cubic bismuth zinc tantalate

C.C. Khaw [a,*], K.B. Tan [b], C.K. Lee [b]

[a] Department of Engineering, Faculty of Engineering and Science, 53300 Universiti Tunku Abdul Rahman, Malaysia
[b] Department of Chemistry, Faculty of Science, 43400 Universiti Putra Malaysia, Malaysia

Received 16 June 2008; received in revised form 8 July 2008; accepted 2 August 2008
Available online 31 August 2008

Abstract

Electrical properties of the parent phase in the Bi_2O_3–ZnO–Ta_2O_5 ternary system, cubic $Bi_{1.5}ZnTa_{1.5}O_7$ (α-BZT), P, are investigated using impedance spectroscopy. P has permittivity (ε′) of 58, dielectric loss (tan δ) of 0.0023 at 30 °C and 1 MHz; temperature coefficient of capacitance (TCC) of −156 ppm/°C in the range of 30–300 °C at 1 MHz. A high degree of dispersion in the permittivity at low frequencies (<1 kHz) and temperatures above 500 °C is apparent. Dielectric losses exhibit non-frequency dependence at low temperatures presenting an increase at temperatures above 500 °C. A decrease of the loss occurs with increasing frequency.

Keywords: Pyrochlore; Permittivity; Dielectric loss; Temperature coefficient of capacitance

1. Introduction

Bismuth-based pyrochlores have been found to be of interest for low-fire high frequency dielectric applications. In contrast to conventional microwave dielectric materials, e.g., $Ba(Mg_{1/3}Ta_{2/3})O_3$ and $Zr(Sn,Ti)O_4$ that require high sintering temperatures ($T_{sinter} > 1600$ K), the low sintering temperatures of bismuth pyrochlores ($T_{sinter} \leq 1400$ K) and dielectric properties with low losses (tan $\delta \sim 10^{-4}$) and dielectric constants up to 150 make them promising candidates for cofired decoupling capacitors in multichip module packaging applications, so called low temperature cofire ceramics (LTCC) packages [1,2,3].

Dielectric properties of $Bi_{1.5}ZnSb_{1.5}O_7$ were investigated by impedance spectroscopy in the frequency range of 5 Hz to 13 MHz; from 100 to 700 °C. The dielectric permittivity dependence as a function of frequency and temperature showed a strong dispersion at frequency lower than 10 kHz. The losses (tan δ) exhibited slight dependence on the frequency at low temperatures and a strong increase at temperature higher than 400 °C [4].

It is now well-established that there are two ternary phases in the bismuth zinc niobate (BZN) system; one is a cubic pyrochlore (α) that forms over a solid solution area that is close to but does not include the so-called ideal composition $Bi_{3/2}ZnNb_{3/2}O_7$ [5,6,7]. This phase has a high permittivity, approximately 150, low dielectric loss, with tan $\delta \approx 0.0005$ at 1 MHz, but a large negative temperature coefficient of capacitance, ~ -500 ppm K^{-1} [8,9,10]. This phase also shows dielectric relaxation at sub-ambient temperatures, with peaks in the permittivity and dielectric loss, which are attributable to polarisation of the pyrochlore crystal lattice associated with off-centre displacement of Bi, Zn cations on the A-sites, linked to off-centre displacement of O′ oxygens [6,11].

The second phase is a monoclinic zirconolite-structured phase (β) of stoichiometry $Bi_2(Zn_{1/3}Nb_{2/3})_2O_7$, although it, too, appears to have a variable composition that, as yet, has not been well characterised. This phase also has a high permittivity, 80, a low dielectric loss, tan δ, ∼0.001, but has a positive temperature coefficient of permittivity, +200 ppm K^{-1} [8,9,10]; however, there is no evidence of any dielectric relaxation in this phase, which is also consistent with its crystal structure, although the Zn atoms do partially occupy split sites. Of particular interest for applications requiring temperature stability of electrical characteristics is to make composites of the cubic pyrochlore and monoclinic zirconolite phases and adjust their relative amounts so that the net temperature coefficient of capacitance is close to zero.

BZN with high permittivity and low dielectric loss has been reported to be a high frequency dielectric material that has

* Corresponding author. Tel.: +60 341079802; fax: +60 341079803.
E-mail address: khawcc@mail.utar.edu.my (C.C. Khaw).

0272-8842/$34.00
doi:10.1016/j.ceramint.2008.08.006

applications in devices such as temperature-stable multilayer ceramics capacitor and microwave resonator and filter [12].

The subsolidus phase diagram of the system Bi_2O_3–ZnO–Ta_2O_5 in the region of the cubic pyrochlore phase (α) has been determined. The pyrochlore solid solutions form a trapezoidal compositional area on the phase diagram, similar in size and location to that of the Nb_2O_5 system, but in this case, it includes the ideal composition $Bi_{1.5}ZnTa_{1.5}O_7$, P [13].

Bi_2O_3–ZnO–Ta_2O_5 system has attracted much attention as new materials with promising microwave properties. Dielectric properties of the two primary phases in BZT, α and β phases as in BZN, were measured using wave guide transmission, ring resonator, resonant post and split cavity at microwave frequencies [14]. Electrical properties of the BZT phases showed similar characteristics to the Nb analogues, with high permittivities, low dielectric losses and opposite signs of the temperature coefficient of permittivity, leading to the possibility of compensation in mixed-phase ceramics. The cubic pyrochlore phase also showed low temperature dielectric relaxation effects, which again were not seen in the monoclinic zirconolite phase [15]. The effect of sintering atmosphere on the structure and dielectric properties of BZT system has been investigated. Sintering atmospheres (in air and in N_2) had little effect on the phase structures of BZT system but the dielectric constants of the samples sintered in N_2 were larger than those sintered in air [16].

Most of the studies in BZT system focused on materials on the join between α and β phase. There is thus far, relatively little information on the detailed high temperature dielectric properties study on cubic pyrochlores in the Bi_2O_3–ZnO–Ta_2O_5 ternary system. Here we report a study on the electrical characteristics of cubic BZT pyrochlore, P, at high temperature.

2. Experimental procedure

Bismuth zinc tantalate materials were prepared by solid-state reaction of mixtures of Bi_2O_3 (99.9%, Aldrich, St. Louis, MO), ZnO (99%, Merck, Darmstadt, Germany), and Ta_2O_5 (99.993%, Alfa-Aesar, Ward Hill, MA); Bi_2O_3 was dried at 300 °C for 1–2 h while ZnO and Ta_2O_5 were dried at 600 °C for 2–3 h prior to weighing. Compositions (3–4 g total) were mixed with acetone in an agate mortar, dried and fired in Pt foil boats at 1050 °C for 2 days, with intermediate regrinding. Weight-loss checks showed no significant loss and therefore no volatilisation of the starting materials. The samples were analysed by X-ray powder diffraction, XRD with a Shimadzu diffractometer XRD 6000, Cu Kα radiation (Kyoto, Japan) to confirm their phase purities. Electrical properties were determined by ac impedance spectroscopy using a Hewlett-Packard Impedance Analyser HP 4192A (Tokyo, Japan) in the frequency range of 5 Hz to 13 MHz. Pellets were cold-pressed and sintered overnight at synthesis temperature, 1050 °C, uncovered with powder and at optimised sintering condition, 1100 °C, covered with sacrificial powder, prior to electrical measurements. All the electrical measurements in this study were done using optimised sintering condition unless otherwise stated in the text. Gold paste electrodes were then fired on at 200–600 °C. Measurements were made from room temperature (~30 °C) to 850 °C by incremental steps of 50 °C on a heating cycle with 30 min equilibration time. The samples were left overnight at ~800 °C and a cooling cycle performed the next day. Most measurements were made in air; however, selected samples were equilibrated in nitrogen at different flow rates to test the oxygen partial pressure, pO_2, dependence of the conductivity.

3. Results and discussion

3.1. Complex impedance study

Fig. 1 shows the complex impedance plots (cole–cole plots) of P at different temperatures. The impedance data are normalised by the geometric factor. The results show that there is a decrease in resistance that may be associated with

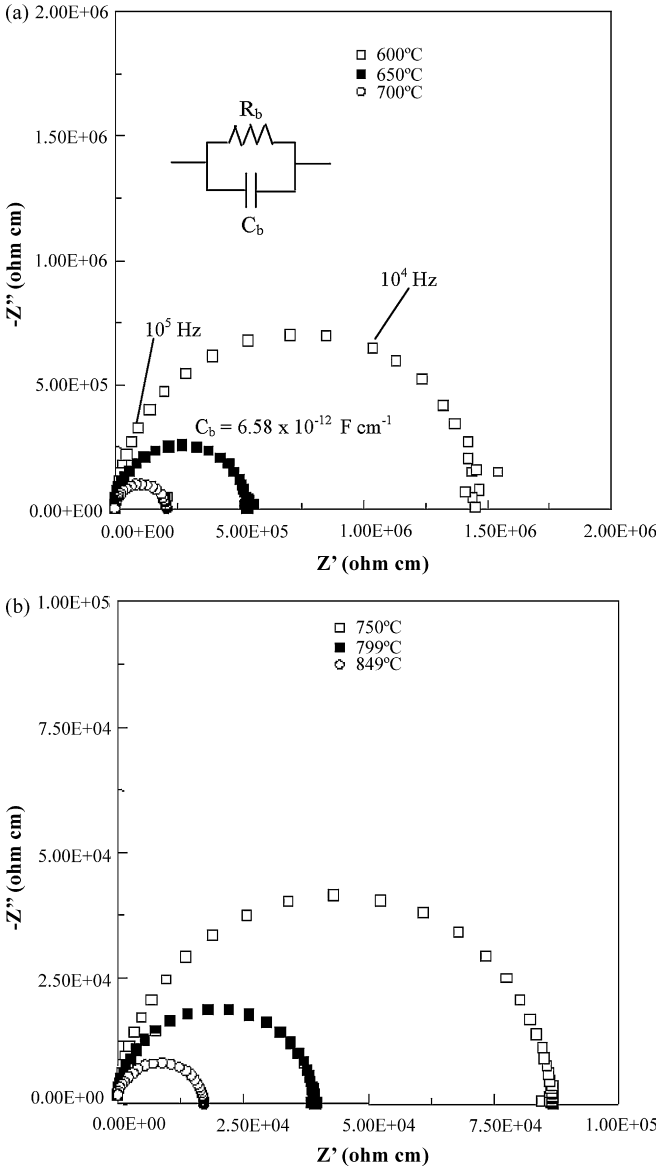

Fig. 1. Cole–cole plots of $Bi_{1.5}ZnTa_{1.5}O_7$ at: (a) 600, 650 and 700 °C; (b) 750, 800 and 850 °C.

intra-granular (bulk) or inter-granular (grain boundary) region of the sample when the temperature of measurements increased. A perfect semicircle is seen in Fig. 1 for measurements at all the temperatures investigated; the associated capacitance at all the temperatures is in the order of 10^{-12} F cm^{-1} (e.g., at 650 °C, the capacitance value is 6.58×10^{-12} F cm^{-1}), which is typical of a bulk material. In the low frequency region, there is no sign of electrode effects (no spike at the intercept of the semicircle with Z' axis (real part of complex impedance)). Therefore, the conducting species are electronic [17]. The impedance data can be represented by the equivalent circuit shown as an inset to Fig. 1, which contains R and C elements of the bulk material, R_b (bulk resistance) and C_b (bulk capacitance), in parallel. This is confirmed by the combined spectroscopic plots shown in Fig. 2. The plots show two coincident peaks of M'' (imaginary part of complex modulus) and Z'' (imaginary part of complex impedance). The half height width of the M'' peak is approximately 1.17 decade, which is closed to the perfect Debye (1.14 decade), indicating that the material is homogenous.

3.2. ac conductivity study

Conductivity values are extracted from cole–cole plots. Conductivities of these materials are reversible on heat–cool cycle. Fig. 3 shows the Arrhenius plots in the logarithmic form of P sintered at 1050 °C and at optimised sintering temperature 1100 °C. Conductivity of P is reversible on heat and cool cycles. Hence only the data from cooling cycles are shown. The results show that the conductivity of the pellet sintered under optimised conditions is slightly higher than that of the pellet sintered at 1050 °C (e.g., at measurement temperature of 650 °C, $\sigma = 5.30 \times 10^{-7}$ ohm^{-1} cm^{-1} with $E_a = 1.57$ eV for pellet sintered at 1050 °C; $\sigma = 6.95 \times 10^{-7}$ ohm^{-1} cm^{-1} with $E_a = 1.55$ eV for pellet sintered at 1100 °C). This is probably

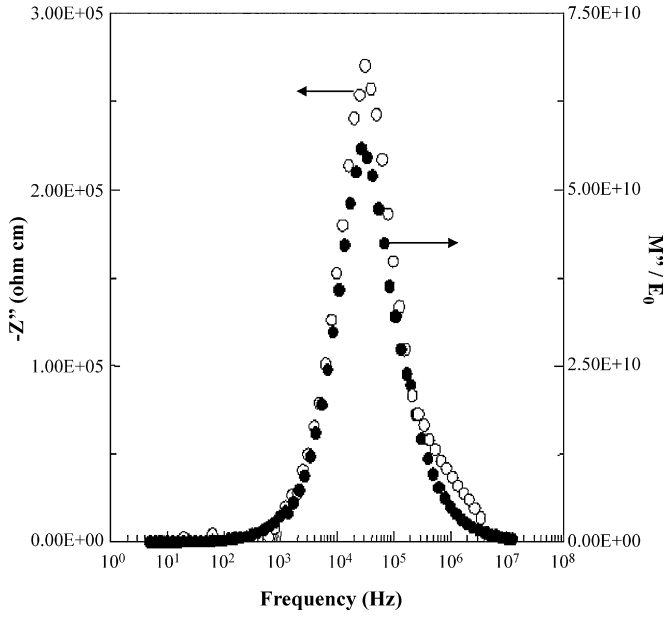

Fig. 2. Combined spectroscopic plots of $Bi_{1.5}ZnTa_{1.5}O_7$ at 650 °C.

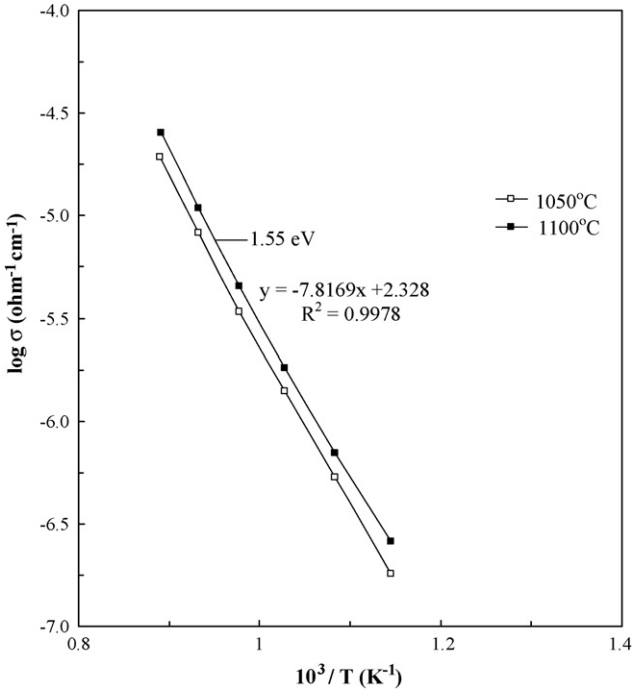

Fig. 3. Arrhenius plots of $Bi_{1.5}ZnTa_{1.5}O_7$ sintered at 1050 and 1100 °C (cooling cycle).

associated with the higher pellet density obtained at higher sintering temperature. Charge carriers can move more easily in the denser pellet with less porosity. The activation energy is higher than that for $Bi_3Zn_2Sb_3O_{14}$ (BZS) (1.37 eV). There is no indication of ionic conduction. High activation values, when not linked to ionic conduction, are usually associated with a hopping type of electronic transport mechanism, which suggests the existence of defects such as oxygen vacancy for the hopping of electrons [18,19].

Fig. 4 shows the imaginary part of impedance as a function of frequency on a logarithmic scale. Dispersion can be seen from the figure and the maxima of the curves are displaced to higher frequencies with the increase in measuring temperature. The presence of a maximum means the presence of a polarisation process. The frequency at the maximum value of each peak was then plotted as an Arrhenius type of plot to represent its dependence on the temperature as shown in Fig. 5. It follows the Arrhenius's law with apparent activation energy, $E_a = 1.54$ eV. This value agrees well with that obtained previously in Fig. 3 ($E_a = 1.55$ eV). The close agreement between these two values indicates that the polarisation phenomenon of the crystalline lattice has a strong influence on the electrical behaviour, providing additional evidence that the conduction mechanism is of the hopping type [18,19].

Fig. 6 shows the modulus spectra, i.e., M'' versus frequency on a logarithmic scale. Peak heights are independent of temperature; peak positions shifted with increase in temperature. It thus appears that P is not ferroelectric. Relaxation time, τ can be obtained from the peak positions since at the peak maximum:

$$\tau = RC = (2\pi f)^{-1} \quad (1)$$

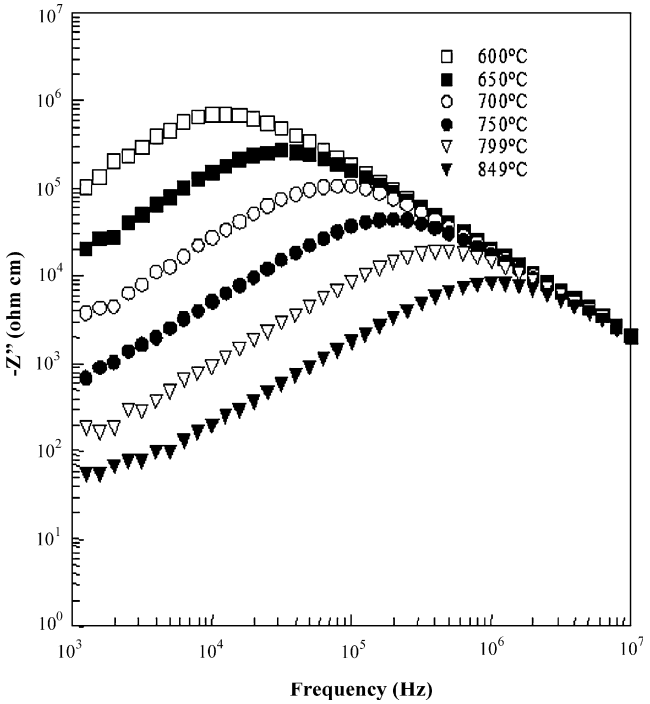

Fig. 4. Imaginary part of impedance of $Bi_{1.5}ZnTa_{1.5}O_7$ at different temperatures as a function of frequency.

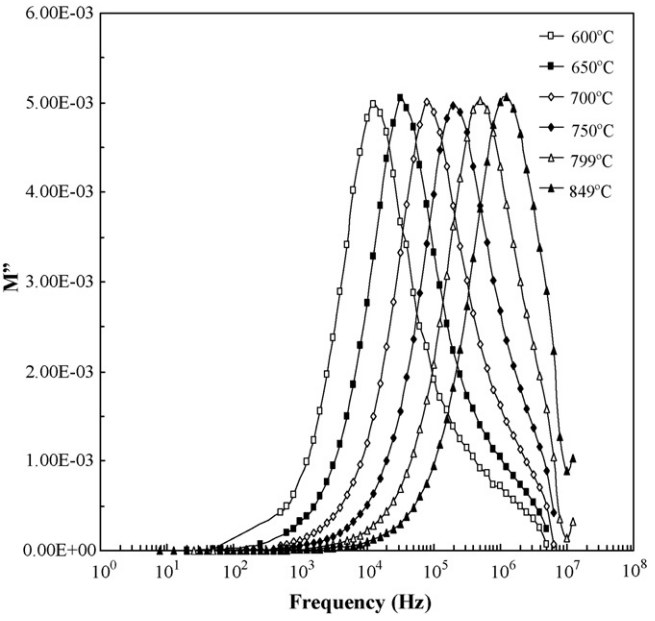

Fig. 6. Modulus plots of $Bi_{1.5}ZnTa_{1.5}O_7$.

An Arrhenius plot of log τ versus 1000/T yields a straight line as shown in Fig. 7 and activation energy calculated from the slope of the graph has a value of E_a = 1.56 eV, which agrees quite well with that obtained previously in Fig. 3 (E_a = 1.55 eV). Therefore, it supports the postulate that the conduction process is a hopping process [20]. The activation energy obtained is higher than that of BZS with E_a = 1.39 eV [4].

The conductivity of P measured in nitrogen atmosphere at a flow rate of 80 cm^3 min^{-1} appeared to have lower conductivity especially at lower temperatures compared to that measured in air (Fig. 8). This indicates that conduction is electronic with p-type semiconductor behaviour. At lower oxygen partial pressures (i.e., in nitrogen atmosphere), it is likely that oxygen is removed from the surface that leads to the generation

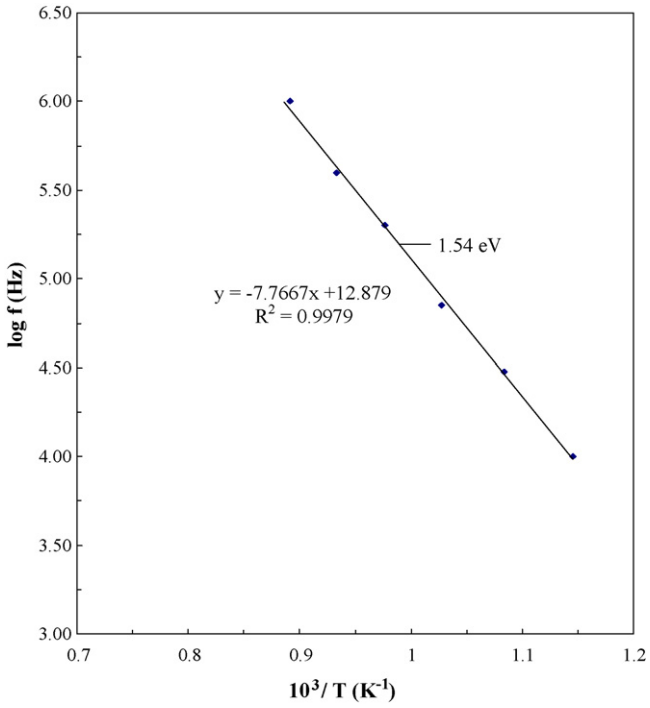

Fig. 5. Arrhenius plot for the peak frequency of $Bi_{1.5}ZnTa_{1.5}O_7$.

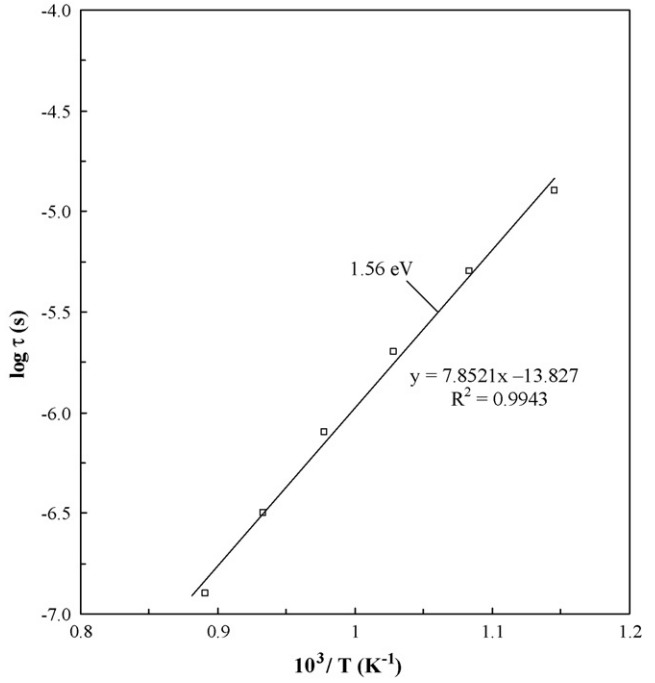

Fig. 7. Arrhenius plot of relaxation time, τ, as a function of reciprocal temperature 1/T.

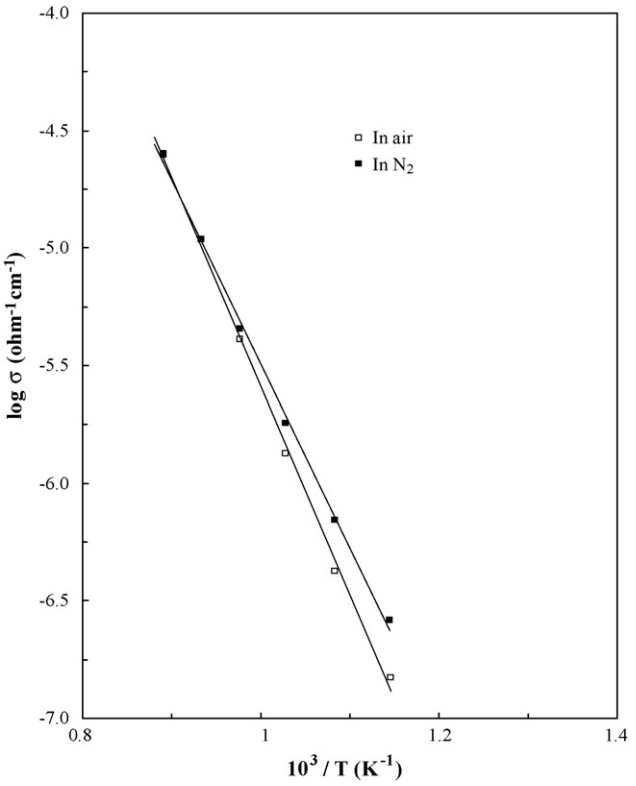

Fig. 8. Arrhenius plots of $Bi_{1.5}ZnTa_{1.5}O_7$ measured in air and in nitrogen (cooling cycle).

of n-type carriers according to the following equation:

$$2O^{2-} \rightarrow O_2 + 4e \quad (2)$$

Since the conductivity of the sample decreases at lower oxygen partial pressures, the principle charge carriers would appear to be holes that are cancelled by the introduction of n-type carriers [21,22].

3.3. Complex permittivity and dielectric loss study

The dielectric properties of P were investigated at various frequencies and temperatures. The permittivity can be expressed as a complex number:

$$\varepsilon^* = \varepsilon' - j\,\varepsilon'' \quad (3)$$

where ε' and ε'' are the real and imaginary parts of the permittivity, respectively. A high degree of dispersion of the permittivity of BZT ceramic at low frequencies (<1 kHz) and temperatures above 500 °C is evident (Figs. 9 and 10). Between 100 and 1000 kHz, non-frequency dependence is observed in the range of 100–300 °C. These behaviours are similar to those observed in BZS ceramic. They are commonly seen in dielectric materials, in which a conduction mechanism of the hopping type is present [4]. The dispersions may be associated with the presence of atomic defects in the structure in which a large number of unoccupied atomic sites is exhibited. This is seen in cubic pyrochlore where oxygen vacancies are an intrinsic defect [23].

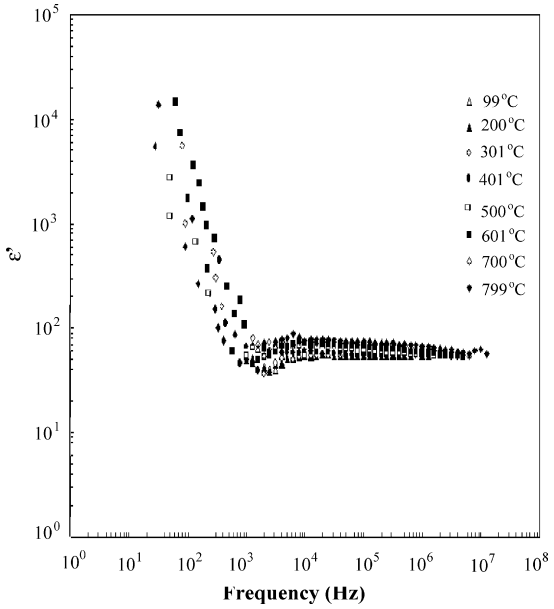

Fig. 9. Real part of complex permittivity as a function of frequency at several temperatures.

Figs. 11 and 12 show the dielectric loss:

$$\tan\delta = \frac{\varepsilon''}{\varepsilon'} \quad (4)$$

as a function of frequency and temperature. In Fig. 11, the curves show an increase of the loss magnitude below 10 kHz.

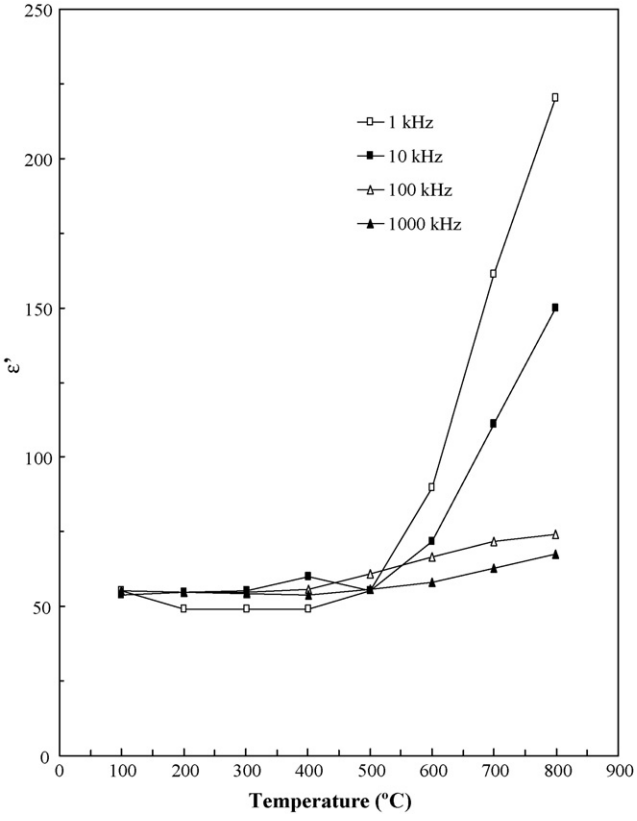

Fig. 10. Real part of complex permittivity as a function of temperature at several frequencies.

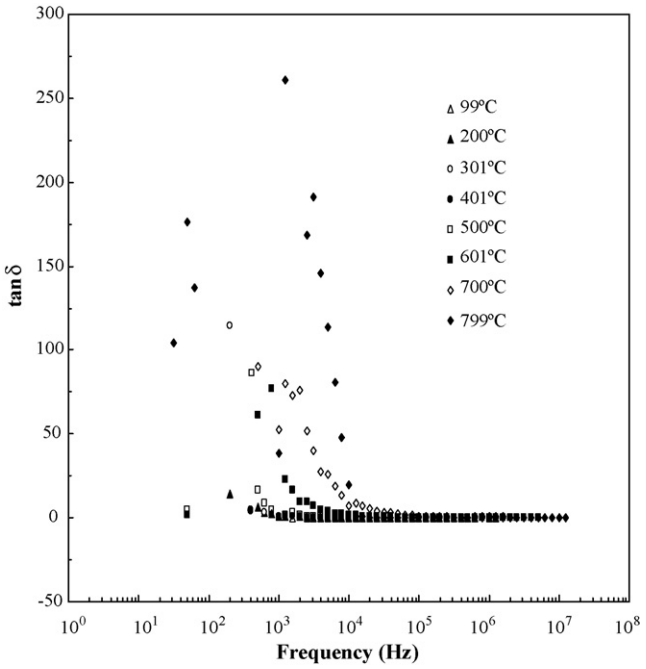

Fig. 11. Dielectric losses, tan δ, as a function of frequency at several temperatures.

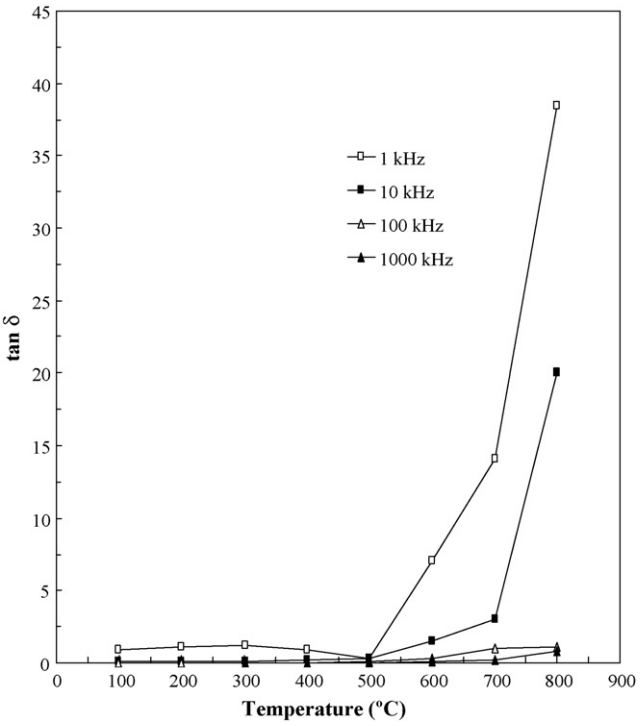

Fig. 12. Dielectric losses, tan δ, as a function of temperatures at several frequencies.

At high frequencies, the losses are much lower than those occurring at low frequencies. This kind of dependence of tan δ with frequency is associated with losses due to the conduction mechanism mentioned earlier. In Fig. 12, dielectric loss decreases with frequencies when temperature is above 500 °C.

On increasing the temperature, the electrical conductivity increases due to the increase in thermally activated drift mobility of electric charge carriers according to the hopping mechanism. Therefore, the dielectric polarisation increases causing a marked increase in ε' and tan δ as temperature increases above 500 °C [24,25]. Both ε' and tan δ decrease with increasing frequency probably because the jumping frequency of electric charge carriers cannot follow the alternation of applied ac electric field beyond a certain critical frequency [24].

The permittivity value of P (sintered at 1100 °C) is 58 at room temperature (30 °C), 1 MHz, smaller than the reported value in literature which is ~71 [15,26]. The permittivity values are, in general, higher than those reported for BZS (~32) but lower than those of bismuth zinc niobate (BZN) ceramics (~150) [1,6,10]. The decrease in permittivity (Nb > Ta > Sb) could be explained by a decrease in the total polarisability or an increase in the molar volume. For example, when Ta is substituted by Sb, there is a decrease in the unit cell volume (lattice constant of BZN > BZT > BZS) and the lower permittivity of BZS may arise from a significant decrease in the total polarisability. It has been reported that dielectrics with high permittivity are based on the structure with BO_6 octahedra joined to one another by their tops. The key ion B located in the centre of octahedra plays an important role in determining dielectric properties. The strong correlation between highly polarisable octahedra not only provides high permittivity, but also brings on critical temperature dependence of permittivity. As to pyrochlore dielectrics, it is believed that there is a strong correlation between octahedra when ions such as Nb^{5+} are placed into the centre of the octahedra and would result in high permittivity. Relatively weak correlation between octahedra when Sb^{5+} is located in the centre brought on low permittivity [27]. Tan δ of α-BZT, P, is 2.3×10^{-3} at 30 °C, 1 MHz. These tan δ values are comparable to those of BZS (10^{-3}) but higher than those of BZN materials (10^{-4}) [1,9].

3.4. Temperature coefficient of capacitance study

The temperature coefficient of capacitance, TCC, is calculated by the following formula:

$$\mathrm{TCC} = \frac{C_{T_2} - C_{T_1}}{C_{T_1}(T_2 - T_1)} \tag{5}$$

where C_{T_1} is the measured capacitance at T_1 (room temperature (~30 °C)), and C_{T_2} is the measured capacitance at T_2 (300 °C) [9].

TCC obtained in this study for P is −156 ppm/°C measured at 1 MHz. This is comparable to the reported value, −172 ppm/°C measured at 1 MHz [15], and is less negative than that of cubic BZN which has a value of ~ −500 ppm/°C [6,9] but more negative than that of cubic BZS (~ −100 ppm/°C) [27]. All the cubic BZT, BZN and BZS have negative values of TCC, which means the capacitance (or permittivity) diminishes with the rise in the low temperature region (100–300 °C in BZT system studied). Large negative TCC (in the case of Nb) and relatively small value of TCC (for Sb) is believed to be related to the strong or weak correlation between octahedra when ions such as Nb or Sb are placed in the centre of the octahedra [27].

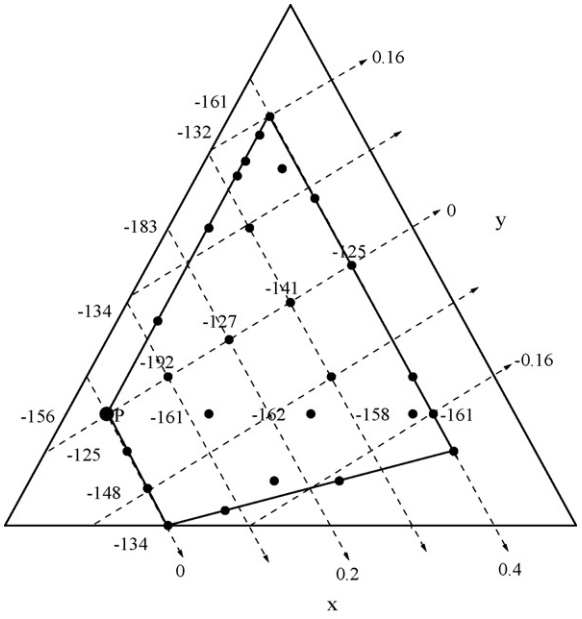

Fig. 13. TCC values within solid solution area of $Bi_{1.5}ZnTa_{1.5}O_7$, P, on (x, y) grid with x and y as variables in the formula, $Bi_{3+y}Zn_{2-x}Ta_{3-y}O_{14-x-y}$.

Valant et al. suggested that a correlation exists between the ratio of the A- and B-site ionic radii (R_A/R_B) and TCC in a chemically substituted α-BZN system; the TCC values decrease as R_A/R_B increase [28]. A similar structure–property correlation which demonstrates the temperature dependence of polarisation on the nature of oxygen octahedra tilting has been established in perovskite-based system [29]. However, in this α-BZT system, TCC values do not show changes with composition within the solid solution series (Fig. 13) [13]; this is consistent with the result of Youn et al. for the study of TCC values within the limited α- and β-BZT solid solution regions [15].

4. Conclusions

Cubic bismuth zinc tantalate (BZT), P, having the composition $(Bi_{1.5}Zn_{0.5})(Ta_{1.5}Zn_{0.5})O_7$ was prepared through the solid-state reaction procedure. The electrical measurements were carried out as a function of frequency and temperature. The complex impedance plots show that P exhibits bulk properties with associated capacitance in the order of 10^{-12} F cm^{-1}. A high degree of dispersion in the permittivity and dielectric loss at low frequency and high temperature suggest that a conduction mechanism of the hopping type is present. Conductivity measurement of P at lower O_2 partial pressure indicates the material to exhibit p-type semiconductor behaviour. Negative TCC values were obtained for pyrochlore materials measured at 1 MHz.

Acknowledgement

We thank Ministry of Science, Technology, and Innovation Malaysia (MOSTI) for financial support via IRPA Grant and NSF scholarship.

References

[1] A. Mergen, W.E. Lee, Crystal chemistry, thermal expansion and dielectric properties of $(Bi_{1.5}Zn_{0.5})(Sb_{1.5}Zn_{0.5})O_7$ pyrochlore, Mater. Res. Bull. 32 (1997) 175–189.
[2] M. Valant, P.K. Davies, Synthesis and dielectric properties of pyrochlore solid solutions in the Bi_2O_3–ZnO–Nb_2O_5–TiO_2 system, J. Mater. Sci. 34 (1999) 5437–5442.
[3] D.P. Cann, C.A. Randall, T.R. Shrout, Investigation of the dielectric properties of bismuth pyrochlores, Solid State Commun. 100 (7) (1996) 529–534.
[4] M.A.L. Nobre, S. Lanfredi, Dielectric spectroscopy on $Bi_3Zn_2Sb_3O_{14}$ ceramic: an approach based on the complex impedance, J. Phys. Chem. Solids 64 (2003) 2457–2464.
[5] K.B. Tan, C.K. Lee, Z. Zainal, G.C. Miles, A.R. West, Stoichiometry and doping mechanism of the cubic pyrochlore phase in the system Bi_2O_3–ZnO–Nb_2O_5, J. Mater. Chem. 15 (2005) 3501–3506.
[6] I. Levin, T.G. Amos, J.C. Nino, T.A. Vanderah, C.A. Randall, M.T. Lanagan, Structural study of an unusual cubic pyrochlore $Bi_{1.5}Zn_{0.92}Nb_{1.5}O_{6.92}$, J. Solid State Chem. 168 (2002) 69–75.
[7] T.A. Vanderah, I. Levin, M.W. Lufaso, A new crystal–chemical principle for the pyrochlore structure, Eur. J. Inorg. Chem. 14 (2005) 2895–2901.
[8] S.M. Zanetti, S.A. Da Silva, G.P. Thin, A chemical route for the synthesis of cubic bismuth zinc niobate pyrochlore nano-powders, J. Solid State Chem. 177 (2004) 4546–4551.
[9] H. Wang, R. Elsebrock, T. Schneller, R. Waser, X. Yao, Bismuth zinc niobate ($Bi_{1.5}ZnNb_{1.5}O_7$) ceramics derived from metallo-organic decomposition precursors solution, Solid State Commun. 132 (7) (2004) 481–486.
[10] X.L. Wang, H. Wang, X. Yao, Structure phase transformations and dielectric properties of pyrochlores containing bismuth, J. Am. Ceram. Soc. 80 (10) (1997) 2745–2748.
[11] R.L. Withers, T.R. Welbury, A.K. Larssen, Y. Liu, L. Noren, H. Rundolf, F.J. Brink, Local crystal chemistry, induced strain and short range order in the cubic pyrochlore BZN, J. Solid State Chem. 177 (2004) 231–244.
[12] H.L. Du, X. Yao, Dielectric relaxation characteristics of bismuth zinc niobate pyrochlores containing titanium, Physica B 324 (2002) 121–126.
[13] C.C. Khaw, C.K. Lee, Z. Zainal, G.C. Miles, A.R. West, Pyrochlore phase formation in the system Bi_2O_3–ZnO–Ta_2O_5, J. Am. Ceram. Soc. 90 (9) (2007) 2900–2904.
[14] H.-J. Youn, C.A. Randall, A. Chen, T.R. Shrout, M.T. Lanagan, Dielectric relaxation and microwave dielectric properties of Bi_2O_3–ZnO–Ta_2O_5 ceramics, J. Mater. Res. 17 (2002) 1502–1506.
[15] H.-J. Youn, T. Sogabe, C.A. Randall, T.R. Shrout, M.T. Lanagan, Phase relations and dielectric properties in the Bi_2O_3–ZnO–Ta_2O_5 system, J. Am. Ceram. Soc. 84 (11) (2001) 2557–2561.
[16] D.S. Peng, L.B. Shen, Y. Zhang, X. Yao, Study on relationship between sintering atmosphere and dielectric properties for Bi_2O_3–ZnO–Ta_2O_5 system, Ceram. Int. 30 (2004) 1199–1202.
[17] D.C. Sinclair, F.B. Morrison, A.R. West, Applications of combined impedance and electric modulus spectroscopy to characterise electroceramics, Ceram. Int. 2 (2000) 33–38.
[18] M.A.L. Nobre, S. Lanfredi, The effect of temperature on the electric conductivity property of $Bi_3Zn_2Sb_3O_{14}$ pyrochlore type phase, J. Mater. Sci.: Mater. Electron. 13 (2002) 235–238.
[19] S. Lanfredi, M.A.L. Nobre, Dielectric dispersion in $Bi_3Zn_2Sb_3O_{14}$ ceramic: a pyrochlore type phase, Mater. Res. 6 (2003) 157–161.
[20] D.P. Almond, A.R. West, Measurement of mechanical and electrical relaxations in β-alumina, Solid State Ionics 3 (1981) 73–77.
[21] C.K. Lee, L.T. Sim, Synthesis and characterisation of modified $LiMn_2O_4$ electrode materials, Malaysian J. Chem. 2 (2002) 27–33.
[22] A.R. West, Crystal defects, non-stoichiometry and solid solutions, in: A.R. West (Ed.), Basic Solid State Chemistry, John Wiley & Sons Ltd., New York, 1999, pp. 226–240.
[23] M.A.L. Nobre, S. Lanfredi, Dielectric properties of $Bi_3Zn_2Sb_3O_{14}$ ceramics at high temperature, Mater. Lett. 47 (2001) 362–366.
[24] H.L. Du, X. Yao, Effects of Sr substitution on dielectric characteristics in $Bi_{1.5}ZnNb_{1.5}O_7$ ceramics, Mater. Sci. Eng. B00 (2003) 1–4.

[25] H.L. Du, X. Yao, H. Wang, Observations on structural evolution and dielectric properties of oxygen-deficient pyrochlores, Ceram. Int. 30 (2004) 1383–1387.
[26] C.A. Randall, J.C. Nino, A. Baker, H.-J. Youn, A. Hitomi, R. Thayer, L.E. Edge, T. Sogabe, D. Anderson, T.R. Shrout, S. Trolier-Mckinstry, M.T. Lanagan, Bi-pyrochlore and zirconolite dielectrics for integrated passive component applications, Am. Ceram. Soc. Bull. (2003) 9101–9108.
[27] H.L. Du, X. Yao, Structural trends and dielectric properties of Bi-based pyrochlores, J. Mater. Sci.: Mater. Electron. 15 (2004) 613–616.
[28] M. Valant, P.K. Davies, Crystal chemistry and dielectric properties of chemically substituted $(Bi_{1.5}Zn_{1.0}Nb_{1.5})O_7$ and $Bi_2(Zn_{2/3}Nb_{4/3})O_7$ pyrochlores, J. Am. Ceram. Soc. 83 (1) (2000) 147–153.
[29] E.L. Colla, I.M. Reaney, N. Setter, Effect of structural changes in complex perovskites on the temperature coefficient of relative permittivity, J. Appl. Phys. 74 (1993) 3414–3425.